Published in final edited form as:
Anal Bioanal Chem. 2010 February ; 396(3): 973. doi:10.1007/s00216-009-2996-1.

Analytical Strategies for Characterizing Nanoparticle's Surface Chemistry

Bin Zhang[1] and **Bing Yan**[1,2,*]

[1]School of Chemistry and Chemical Engineering, Shandong University, Jinan 250100, China

[2]St. Jude Children's Research Hospital, Memphis, TN 38105, U.S.A.

Abstract

Chemical modifications of nanoparticle (NP) surface are likely to regulate their activities, remove their toxic effects, and enable them to perform desired functions. It is urgent to develop analytical strategies for acquiring structural and quantitative information on small molecules linked to the surface of NP. Recent progresses on characterizing nanoparticle's surface chemistry using nuclear magnetic resonance spectroscopy (NMR), Fourier transform infrared absorbance spectroscopy (FTIR), liquid chromatography-mass spectroscopy (LC-MS), X-Ray photoelectron spectroscopy (XPS), and combustion elemental analysis are reviewed.

Keywords

nanoparticle; NMR; FTIR; MS; XPS; combustion elemental analysis

Large surface areas of nanomaterials control their biological activities. Early studies suggested that cellular responses to nanomaterials modified by surface coating molecules reflect the adsorbed molecular layer, rather than the material itself [1–3]. Chemical modifications of nanoparticle (NP) surface are likely to regulate their activities, remove their toxic effects, and enable them to perform desired functions [4]. Two recent reports used parallel chemical modifications [5] of magnetic NPs and combinatorial chemical modifications [6] of multi-walled carbon nanotubes (MWNTs) and showed that careful design and modification of surface chemistry of NPs can control their biological activity and improve their biocompatibility.

Modified NPs need to be characterized rigorously regarding the integrity of the chemistry. However, identification and quantification of small molecules linked to the surface of NPs are very challenging due to the fact that they are solid-phase samples and they are coated with only a small amount of small molecules. This has become a roadblock limiting our ability to do chemical modifications of nanomaterials. For this technical difficulty, many previous publications did not thoroughly characterize modified NPs before doing biological testing. On the other hand, biological experiments require precise quantity/ concentration information to obtain dose-response relationship. The lack of accurate concentration information makes the biological studies qualitative at best.

Recently, efforts have been made to fill this gap. In this review, we focus on recent development of multiple analytical techniques, such as nuclear magnetic resonance spectroscopy (NMR), Fourier transform infrared absorbance spectroscopy (FTIR), liquid chromatography-mass spectroscopy (LC-MS), X-Ray photoelectron spectroscopy (XPS), and combustion elemental

901-495-2797, Dr.bingyan@gmail.com.

analysis and explain how these techniques help identify and quantify molecules attached to NP's surface. The continued efforts in this field will pave the way to make the wider biomedical application of nanomaterials possible.

1. Nuclear Magnetic Resonance Spectroscopy (NMR)

1.1 Solution ^{1}H NMR of nanomaterials attached molecules

NMR has been used as a gold standard for structural characterization of organic molecules. For NPs with good solubility, it is possible to study the surface-bound molecules directly using solution ^{1}H NMR technique. Studies of thiophenol-coated cadmium sulfide (CdS) QDs [7–11], 2-carboxyethanephosphonic acid coated SnO_2 NPs [12] and oleic acid coated iron-oxide NPs [13] have been reported. However, the power of solution NMR is often negated by nanomaterials' low solubility and inhomogeneity. When attached to a solid particle, the individual molecules cannot tumble rapidly to average the signal to give sharp NMR signals as in solution [14–23]. Such a phenomenon was well illustrated in Figure 1, in which the solution ^{1}H NMR signals of molecule bound to single-walled carbon nanotubes (SWNTs) were broad [17], and not all protons' signals were detected (Figure 1 bottom) compared with NMR signals of molecule alone in solution (Figure 1 top).

Coupling molecules to NPs through a long, flexible, solvable linker can enhance NPs' solubility and thus can generally improve their NMR spectra. However, in reality, building such structures into the desired molecules is a synthetic challenge. Therefore, we found that routine NMR spectroscopy can monitor reaction and the product formation, but is not an ideal method for full structure elucidation of organic molecules on the surface of NPs [24].

1. 2 Indirect quantitative assessment of surface-bound ligands on Au NP by ^{1}H NMR

Although solution ^{1}H NMR spectroscopy of the Au NPs could be used to follow the extent of reaction on their monolayers, quantification of ligand exchange can be difficult due to the NMR peaks' significant broadening by attachment to particle surfaces [25]. An alternative strategy is to cleave the alkanethiols from the Au NPs by oxidation with iodine and to subsequently analyze the relative quantities of the solution phase ligands using ^{1}H NMR spectroscopy [26]. Comparison of the peak integrations from the NMR spectra as a function of reaction enables an estimation of the percentages of surface-bound ligands per Au NP. Assuming that (a) no ligands are destroyed through side reactions and (b) all ligands are completely cleaved from the surface upon reaction with I_2, the intensities of the peaks in the NMR spectra are proportional to their relative concentrations on the Au NPs' surfaces [27]. This indirect assessment of cleaved products by ^{1}H NMR can be not only used to obtain purity and structure information of surface-bound ligands on Au NP, but also can be used to monitor conversions during multi-step modifications. The drawbacks of this method are that it is time consuming and destructive [28,29].

1.3 Magic-angle spinning (MAS) NMR spectroscopy

MAS NMR spectroscopy is reported to characterize the structural and dynamic properties of NPs, whereas ^{13}C NMRspectroscopy gives information about the alkyl chain conformation and mobility, and ^{31}P NMR spectroscopy is a sensitive probe of the local environment of phosphorus-containing functional groups. ^{13}C and ^{31}P NMR has been used to study the attached small molecules on gold clusters [27,30–34], carbon nanotubes (CNTs) [35,36], and quantum dots [37]. Gold NPs capped with 11-mercaptoundecanylphosphonic acid (MUP) were synthesized and characterized by MAS NMR spectroscopy [33]. The solution ^{1}H NMR spectrum of the gold colloids showed no signal. At pH 10, where the phosphonate groups are expected to be deprotonated, the chain mobility is sufficiently restricted to completely broaden the NMR resonances. A similar phenomenon was observed for carboxylic acid- and hydroxyl-

functionalized gold NPs [32,33]. The ^{13}C CP/MAS NMR spectrum of MUP adsorbed on gold NPs is shown in Figure 2c along with the solution (Figure 2a) and the MAS (Figure 2b) ^{13}C NMR spectra of the unbound MUP. Small peaks can also be shadowed by the adjacent large peaks. These drawbacks prevent a full structural characterization.

Proton high-resolution magic-angle spinning ^{1}H (HRMAS) NMR technique, successfully used in late 1990s for applications in combinatorial chemistry [38–45], has evolved to be a method to characterize samples with limited amount or semisolid biological samples such as whole cells and tissues [46–49]. By spinning the sample at the magic angle (54.7° relative to the direction of main magnetic field), line broading contributions from magnetic susceptibility and chemical shift anisotropy to the NMR spectra are significantly reduced [50]. An efficient method was developed to make carbohydrate- and protein-coated MNPs via a surface diazo transfer/azide-alkyne click chemistry. Well-resolved ^{1}H NMR signals at 8.0 ppm for all modified MNPs confirmed the presence of triazole protons [51].

A multi-walled carbon nanotubes (MWNTs)-combinatorial library was synthesized. ^{1}H HRMAS NMR was used for structural confirmation [6]. Different MWNTs sharing the same benzenesulfonyl group had similar aromatic proton signals at 7.29–7.94 ppm. MWNTs sharing the same 3-nitro-benzenesulfonyl group had NMR peaks at 7.64–7.81 ppm due to the reduced electron density by nitro group substitution.

^{13}C, ^{29}Si, and ^{31}P MAS NMR were also reported to show distinct resonances for siloxane and other organic moieties on silica [52,53] and gold NPs [54–57]. However, these reports were mainly about identification of special functional groups, instead of full structural elucidation. The ^{1}H MAS NMR spectra of GNPs using 40 μL nanoprobe with water suppression can provide nearly solution-like quality. By effectively optimizing ^{1}H high resolution MAS NMR conditions and applying one- and two-dimensional techniques (1-D and 2-D NMR), ligand structures on surfaces of gold NPs (GNPs) were fully characterized [58]. Significant differences were also found in detection sensitivity depending on the distance between the surface of GNP and protons in the ligand molecule, with the loss of sensitivity for protons closer to the NPs consistent with other report [59]. Figure 3 shows the ^{1}H NMR spectra for the free ligands (spectra a, d, g, j), ^{1}H NMR spectra of GNPs (b, e, h, k), and ^{1}H HRMAS NMR spectra of GNPs **1**–**4** (c, f, i, l) [58].

2-D HRMAS NMR was also performed to elucidate ligands structures on these GNPs' surface. Correlation spectroscopy (COSY), total correlation spectroscopy (TOCSY) and heteronuclear single quantum coherence (HSQC) spectra for GNP **3** were shown in Figure 4. Molecules attached on GNP **3** can be elucidated on the basis of COSY, TOCSY, HSQC and 1-D NMR data [58]. These results demonstrated that ^{1}H HRMAS NMR is an irreplaceable method for a full characterization of molecules bound to NP's surface.

Furthermore, the investigation showed that NMR spectra of aromatic protons in ligands attached to GNP seem to have a broad base compared with aliphatic ligands, indicating the π-π stacking effects.

2. Fourier Transform Infrared Absorbance Spectroscopy (FTIR)

FTIR has been used to identify functional groups on molecules that are attached to NPs [6, 60–62]. Au-MCH (MCH = 6-mercapto-1-hexanol, HS-$(CH_2)_6$-OH) nanoclusters were synthesized [63]. The OH terminal group of the MCH ligand has been directly functionalized through chemical reactions to generate products such as ester or carbamate, as monitered by FTIR spectroscopy. The FTIR spectrum of solid Au-MCH in Figure 5A shows similarity to that obtained for the pure MCH molecule except that the SH vibrational band at 2550 cm^{-1} has disappeared after binding to Au surface. The FTIR spectrum of the Au NPs after

esterification with CF_3COOH (Figure 5B) contains a new intense vibrational band at 1787 cm^{-1}. This is assigned to the CO stretch of the -COO ester group. Peak at 2106 cm^{-1} (Figure 5C) belongs to the characteristic peak of N=C=S stretch (at 2143 cm^{-1} for pure NCO-C_6H_4-NCS solid).

In another report [27], the surface of Au NPs was modified with triazole cycloaddition through "click" chemistry. Azide-functionalized Au NPs were reacted with a series of alkynyl molecules. Au particle samples were first synthesized through standard procedures, the methyl-terminated chains partially exchanged with ω-bromo-functionalized thiol, and the Br termini converted to azides by reaction with NaN_3 (Scheme 1). The FTIR spectrum of the alkanethiol stabilized particles (Figure 6, solid line) is relatively featureless and contains characteristic alkyl stretching vibrations between 2800 and 3000 cm^{-1}, and indicate that the alkyl chains are well-ordered. In comparison, the FTIR spectrum of the Au NPs that have reacted with NaN_3 (Figure 6, dashed line) contains a strong, new vibrational band at 2094 cm^{-1} that is attributed to the cumulated double bonds of the terminal azide moiety. The characteristic alkyl stretching vibrations are not significantly affected (versus the methyl-terminated particles), suggesting that ligand exchange and N_3 substitution do not perturb the structure of the monolayer.

Cycloaddition reactions can also be utilized to prepare multifunctional Au NPs by simultaneously stirring the N_3-terminated NPs with several acetylenic small molecules. To demonstrate this, N_3-containing Au NPs was reacted with a solution containing both the ferrocene (Fc) and the nitrobenzene (NB) propyn-1-one species. The FTIR spectrum of the resultant particles (Figure 7) contains vibrations between 1500 and 1700 cm^{-1} due to C=O and triazole ring stretching modes. Although it is complex, the spectrum indicates the existence of a multifunctional Au NP containing both Fc and NB species linked through triazole ring formation.

Utilizing a nano-combinatorial library strategy, we [6] have constructed a novel surface-modified MWNTs library containing 80 members (Scheme 2), and aimed to discover novel f-MWNTs with reduced protein binding, cytotoxicity, and immune responses through multiple biological screenings. Surface chemistry structures of all the members from the library were characterized by FTIR. Figure 8 is FTIR spectra of f-MWNTs [5],[6],[7],[8], and [9]. When pristine MWNT was oxidized, an IR band at 1713 cm^{-1} appeared indicating the formation of carboxylic acid groups. MWNT **6** reacted with Fmoc-tyrosine and the IR bands of phenol ester carbonyl and carboxylic acid of tyrosine overlapped at ~ 1710 cm^{-1}. The amidation of **7** produced **8**, which was characterized by disappearance of an acid carbonyl band at 1710 and the formation of bands at 2843 and 2924 cm^{-1}. Final product synthesis induced further IR changes. In the case of f-MWNT **9**, an ester carbonyl band at 1787 cm^{-1} emerged due to an ester group on its building blocks.

3. Mass Spectroscopy (MS)

A MS approach was reported to chracterize ZnO NPs modified with Acrylic acid (AA) by plasma polymerization [64]. Figure 9a shows the positive and negative time of flight secondary ion mass spectroscopy (TOFSIMS) of coated ZnO NPs. The spectra in the positive ion mode show strong peaks related to molecular fragments such as $C_4H_7^+$, $C_4H_9^+$, $C_6H_{13}O_4$, $C_7H_9COH^+$, and $C_7H_9COOH^+$. The spectra in the negative ion mode show the existence of the AA (acrylic acid) monomer, AA dimer, AA dimmer + C_2H_4 and AA dimmer + C_3H_6.

Functionalized CNTs have been used as the MALDI matrix [65–68] for the study of small molecules and macromolecules. CNTs was derivatized with iminodiacetic acid (IDA), which could chelate Cu^{2+} [69]. These Cu^{2+} loaded CNTs was used as biomarkers for the selective binding of biomolecules from a complex sample such as serum. Peptides and proteins, bound to the surface of the derivatized CNTs, were then directly analyzed by matrix assisted laser

desorption ionisation/time of flight mass spectrometry (MALDI/TOFMS). The protein mass fingerprinting are the characteristic for every serum sample that may be utilized as disease markers.

Mass spectroscopy could also be used to monitor the synthesis of gold NPs (GNPs). GNPs with diameter of 5–6 nm was synthesized through the reduction reaction using sodium borohydride (SBH) in the presence of mono-6-deoxy-6-pyridinium-β-cyclodextrin chloride (p-βCD) [70]. A reaction intermediate was detected during the reaction process by MS. After 1 min, the p-βCD was already converted to its reduced form, as confirmed by the presence of protonated ion at m/z 1201 and its corresponding sodium adduct at m/z 1223 (Figure 10). As the reaction proceeded, the relative intensities of ions at m/z 1201 vs 1197 decreased. After 90 min, the ion at m/z 1201 almost disappeared. Such data confirmed that the oxidized p-βCD was reduced by SBH as an intermediate (m/z 1201), which was slowly reoxidized to its original form.

We have used thioctic acid and its derivatives for chemical modification of GNPs. When the GNPs are oxidized in the presence of I_2, the free ligand can be cleaved from the surface of GNPs. The loading of multiple ligands can be quantified by LC/MS/UV/CLND to analyze the ratio of ligands in multiple functionalized GNPs (manuscript submitted).

4. X-Ray Photoelectron Spectroscopy (XPS)

XPS can provide information on elemental composition [71,72]. In an early study [73], XPS was used to elucidate the chemical species of acid-oxidized MWNTs. C_{1s} XPS spectra indicated that peaks with higher binding energies located at 286.2, 287.5, and 288.9 eV are assigned to carbon atoms bound to one, two, and three oxygen atoms, respectively. Hence, they can be assigned as >CH-O- (e.g., alcohol, ether), >C=O (ketone, aldehyde), and -COO- (carboxylic acid, ester) species, respectively.

SWNT was functionalized by the addition of (R-)-oxycarbonyl nitrenes which allows for the covalent binding of a variety of different groups such as alkyl chains, aromatic groups, dendrimers, crown ethers, and oligoethylene glycol units [74]. XPS was used to determine the elemental composition of the functionalized SWNT. From the comparison between the spectra of the SWNT starting material and reaction products, characteristic conversions can be confirmed. A detailed analysis of various reaction products was made through the spectrum of C_{1s} and O_{1s} (Figure 11), and the amount of nitrogen and carbon in the sample.

In another report [75], interaction between surface-bound alkylamines and gold NPs were studied using XPS. From the presence of two chemically distinct Cl 2p components it was concluded that both $AuCl_4^-$ and $AuCl_2^-$ ions existed on the surface of gold NPs. Results lead to a conclusion that two modes of binding between alkylamines and the gold surface was confirmed. The loosely bound component is attributed to the formation of an electrostatic complex between protonated amine molecules and surface-bound $AuCl_4^-/AuCl_2^-$ ions, while species with stronger binding was tentatively assigned to $[AuCl(NH_2R)]$.

5. Combustion Elemental Analysis

Combustion elemental analysis has been used in the quantitative analysis of chemical modification of NPs [6,35,58,76,77]. By analyzing the percentage of C, N, S and H elements in modified and unmodified NPs, one can get the quantitative information on the surface composition of NPs.

Surface modification of silica-coated magnetite NPs with (aminopropyl) triethoxysilane (APTS) was analyzed by elemental analysis to optimize the reaction conditions such as solvent,

reaction temperature and reaction time [76]. The effect of reaction variables on the final product was quantified in terms of C, H and N elemental analysis of the loaded molecules. Relative high percentage of C, H and N content was found if the reaction was performed in THF indicating that more APTS molecules were bound to the NP's surface. An IR band at 790 cm^{-1} corresponding to NH_2 bending modes of the APTS molecule also confirmed such reactions.

A method for the modification of amine groups onto the surface of magnetite and silica-coated magnetite NPs was developed based on the condensation of aminopropyltriethoxysilane [77]. From the elemental analysis results, the organic content of the starting material is very low. After modification, a higher percentage of N was detected in all NPs. The amine density determined by this method lies between 42 to 78 μmol g^{-1} depending on the conditions used for the synthesis.

We have designed and synthesized a functionalized MWNTs library using carboxylated MWNT as starting material. We have used several analytical methods to characterize the starting material and the f-MWNT library. By derivatizing carboxylic acid group into amide and performing elemental analysis, we determined that the loading of carboxyl group is 0.45 mmol g^{-1} [6].

6. Concluding Remarks

Analytical strategies for identification and quantification of NP's surface chemistry are crucial for modulating NP's biological activities and toxicity. NMR and FTIR play important roles in the structure confirmation of functional group bound to NPs. Although Solution NMR, MAS NMR and HR MAS NMR can be used to identify structural components of different functionalized NPs, 1-D and 2-D HRMAS NMR measurements are irreplaceable methods for structure elucidation of NP's surface-bound molecules. Furthermore, NMR and FTIR techniques can be also used to monitor the reaction conversions for the multi-step modifications. XPS and elemental analysis are techniques for determining the chemical compositions of molecules bound to NPs. LC/MS analysis after ligand cleavage is the only method for qualitative and quantitative analysis of multiple functionalized NPs, when a quantitative detector such as CLND is used.

It is highly promising that NPs may have more and more applications in therapy, medicine delivery, and diagnosis. The unusual large surface area of NPs suggests that surface chemical modification would play a critical role in modulating their toxicity and biological specificity both in vitro and in vivo. It is not surprising to witness more focused and diverse chemical modifications of nanomaterial surface in future research. However, reliable characterization on the identity and quantity of surface attached molecules for different nanomaterials remain a bottleneck. Although significant progresses have been made on analytical strategies for nanomaterials surface chemistry, identifying the attached molecules and quantifying their loading still require our continued dedication and efforts.

Acknowledgments

This work was supported by Shandong University, St. Jude Children's Research Hospital and the American Lebanese Syrian Associated Charities (ALSAC).

References

1. Lynch I, Dawson KA, Linse S. Sci STKE 2006;327:14–19.
2. Norde W, Lyklema J. J Biomater Sci Polym Ed 1991;2:183. [PubMed: 1854684]
3. Gray JJ. Curr Opin Struct Biol 2004;14:110–115. [PubMed: 15102457]

4. Hong R, Fischer NO, Verma A, Goodman CM, Emrick T, Rotello VM. J Am Chem Soc 2004;126:739–743. [PubMed: 14733547]
5. Weissleder R, Kelly K, Sun EY, Shtatland T, Josephson L. Nat Biotechnol 2005;23:1418–1423. [PubMed: 16244656]
6. Zhou HY, Mu QX, Gao NN, Liu AF, Xing YH, Gao SL, Zhang Q, Qu GB, Chen YY, Liu G, Zhang B, Yan B. Nano Lett 2008;8:859–865. [PubMed: 18288815]
7. Sachleben JR, Wooten EW, Emsley L, Pines A, Colvin VL, Alivisatos AP. Chem Phys Lett 1992;198:431–436.
8. Sachleben JR, Colvin V, Emsley L, Wooten EW, Alivisatos AP. J Phys Chem B 1998;102:10117–10128.
9. Lippens PE, Lannoo M. Phys Rev B: Condens Matter 1989;39:10935–10942. [PubMed: 9947904]
10. Majetich SA, Carter AC, Belot J, McCullough RD. J Phys Chem 1994;98:13705–13710.
11. Diaz D, Rivera M, Ni T, Rodriguez JC, Gastillo-Blum SE, Nagesha D, Robles J, Alvarez-Fregoso OJ, Kotov NA. J Phys Chem B 1999;103:9854–9858.
12. Holland GP, Sharma R, Agola JO, Amin S, Solomon VC, Singh P, Buttry DA, Yarger JL. Chem Mater 2007;19:2519–2526.
13. Willis AL, Turro NJ, O'Brien S. Chem Mater 2005;17:5970–5975.
14. Wang Z, Liu Q, Zhu H, Liu H, Chen Y, Yang M. Carbon 2007;45:285–292.
15. Lin Y, Rao AM, Sadanadan B, Kenik EA, Sun Y-P. J Phys Chem B 2002;106:1294–1298.
16. Hong C-Y, You Y-Z, Pan C-Y. Polymer 2006;47:4300–4309.
17. Sun Y-P, Fu K, Lin Y, Huang W. Acc Chem Res 2002;35:1096–1104. [PubMed: 12484798]
18. Barrientos AG, de la Fuente JM, Rojas TC, Fernández A, Penadés S. Chem Eur J 2003;9:1909–1921.
19. Alvaro M, Aprile C, Ferrer B, Garcia H. J Am Chem Soc 2007;129:5647–5655. [PubMed: 17411044]
20. Gibson JD, Khanal BP, Zubarev ER. J Am Chem Soc 2007;129:11653–11661. [PubMed: 17718495]
21. Zhang Y, Zhang J. J Colloid Interf Sci 2005;283:352–357.
22. Murakami Y, Konishi K. J Am Chem Soc 2007;129:14401–14407. [PubMed: 17967018]
23. Foos EE, Snow AW, Twigg ME, Ancona MG. Chem Mater 2002;14:2401–2408.
24. Du FF, Zhou HY, Chen LX, Zhang B, Yan B. Trends in Anal Chem 2009;28:88–95.
25. Terrill RH, Postlethwaite TA, Chen C, Poon CD, Terzis A, Chen A, Hutchison JE, Clark MR, Wignall G, Londono JD, Superfine R, Falvo M, Johnson CS, Samulski ET, Murray RW. J Am Chem Soc 1995;117:12537–12548.
26. Templeton AC, Hostetler MJ, Kraft CT, Murray RW. J Am Chem Soc 1998;120:1906–19911.
27. Fleming DA, Thode CJ, Williams ME. Chem Mater 2006;18:2327–2334.
28. Rowe MP, Plass KE, Kim K, Kurdak C, Zellers ET, Matzger AJ. Chem Mater 2004;16:3513–3517.
29. Tan H, Zhan T, Fan WY. J Phys Chem B 2006;110:21690–21693. [PubMed: 17064127]
30. Song Y, Harper AS, Murray RW. Langmuir 2005;21:5492–5500. [PubMed: 15924480]
31. Zelakiewicz BS, de Dios AC, Tong YY. J Am Chem Soc 2003;125:18–19. [PubMed: 12515490]
32. Badia A, Gao W, Singh S, Demers L, Cuccia L, Reven L. Langmuir 1996;12:1262–1269.
33. Schmitt H, Badia A, Dickinson L, Reven L, Lennox RB. Adv Mater 1998;10:475–480.
34. Fiurasek P, Reven L. Langmuir 2007;23:2857–2866. [PubMed: 17309224]
35. Zhu Y, Peng AT, Carpenter K, Maguire JA, Hosmane NS, Takagaki M. J Am Chem Soc 2005;127:9875–9880. [PubMed: 15998093]
36. Xu M, Zhang T, Gu B, Wu JL, Chen Q. Macromolecules 2006;39:3540–3545.
37. Berrettini MG, Braun G, Hu JG, Strouse GF. J Am Chem Soc 2004;126:7063–7070. [PubMed: 15174877]
38. Anderson RC, Jarema MA, Shapiro MJ, Stokes JP, Ziliox M. J Org Chem 1995;60:2650–2651.
39. Anderson RC, Stokes JP, Shapiro MJ. Tetrahedron Lett 1995;36:5311–5314.
40. Wehler T, Westman J. Tetrahedron Lett 1996;37:4771–4774.
41. Keifer PA, Baltusis L, Rice DM, Tymiak AA, Shoolery JN. J Magn Reson, Ser A 1996;119:65–75.
42. Shapiro MJ, Chin J, Marti RE, Jarosinski MA. Tetrahedron Lett 1997;38:1333–1336.

43. Keifer PA. Drug Discovery Today 1997;2:468–478.
44. Warrass R, Wieruszeski JM, Boutillon C, Lippens G. J Am Chem Soc 2000;122:1789–1795.
45. Warrass R, Lippens G. J Org Chem 2000;65:2946–2950. [PubMed: 10814182]
46. Taylor JL, Wu CL, Cory D, Gonzalez RG, Bielecki A, Cheng LL. Magn Reson Med 2003;50:627–632. [PubMed: 12939772]
47. Keshari KR, Zektzer AS, Swanson MG, Majumdar S, Lotz JC, Kurhanewicz J. Magn Reson Med 2005;53:519–527. [PubMed: 15723415]
48. Li W, Lee REB, Lee RE, Li JH. Anal Chem 2005;77:5785–5792. [PubMed: 16159107]
49. Li W. Analyst 2006;131:777–781. [PubMed: 16874945]
50. Weybright P, Millis K, Campbell N, Cory DG, Singer S. Magn Reson Med 1998;39:337–345. [PubMed: 9498588]
51. Polito L, Monti D, Caneva E, Delnevo E, Russo G, Prosperi D. Chem Commun 2008;5:621–623.
52. Sadasivan S, Khushalani D, Mann SJ. Mater Chem 2003;13:1023–1029.
53. Bauer F, Glasel HJ, Hartmann E, Bilz E, Mehnert R. Nucl Instrum Methods Phys Res B 2003;208:267–270.
54. Badia A, Lennox RB, Reven L. Acc Chem Res 2000;33:475–481. [PubMed: 10913236]
55. Badia A, Demers L, Dickinson L, Morin FG, Lennox RB, Reven L. J Am Chem Soc 1997;119:11104–11105.
56. Pawsey S, Yach K, Reven L. Langmuir 2002;18:5205–5212.
57. Fiurasek P, Reven L. Langmuir 2007;23:2857–2866. [PubMed: 17309224]
58. Zhou HY, Du FF, Li X, Zhang B, Li W, Yan B. J Phys Chem C 2008;112:19360–19366.
59. Kohlmann O, Steinmetz WE, Mao XA, Wuelfing WP, Templeton AC, Murray RW, Johnson CS. J Phys Chem B 2001;105:8801–8809.
60. Zhu YH, Peng AT, Carpenter K, Maguire JA, Hosmane NS, Takagaki M. J Am Chem Soc 2005;127:9875–9880. [PubMed: 15998093]
61. Nidumolu BG, Urbina MC, Hormes J, Kumar C, Monroe WT. Biotechnol Prog 2006;22:91–95. [PubMed: 16454497]
62. Yoo BK, Joo SW. J Colloid Interface Sci 2007;311:491–496. [PubMed: 17434180]
63. Tan H, Zhan T, Fan WY. J Phys Chem B 2006;110:21690–21693. [PubMed: 17064127]
64. Shi D, He P. Rev Adv Mater Sci 2004;7:97–107.
65. Ren SF, Zhang L, Cheng ZH, Guo YL. J Am Soc Mass Spectrom 2005;16:333–339. [PubMed: 15734326]
66. Chen WY, Wang LS, Chiu HT, Chen YC, Lee CY. J Am Soc Mass Spectrom 2004;15:1629–1635. [PubMed: 15519230]
67. Ugarov MV, Egan T, Khabashesku DV, Schultz JA, Peng H, Khabashesku VN, Furutani H, Prather KS, Wang H-WJ, Jackson SN, Woods AS. Anal Chem 2004;76:6734–6742. [PubMed: 15538798]
68. Xu S, Li Y, Zou H, Qiu J, Guo Z, Guo B. Anal Chem 2003;75:6191–6195. [PubMed: 14616000]
69. Najam-ul-Haq M, Rainer M, Schwarzenauer T, Huck CW, Bonn GK. Anal Chim Acta 2006;561:32–39.
70. Male KB, Li J, Bun CC, Ng S-C, Luong JHT. J Phys Chem C 2008;112:443–451.
71. Li J, Vergne MJ, Mowles ED, Zhong WH, Hercules DM, Lukehart CM. Carbon 2005;43:2883–2893.
72. Lee J, Yang J, Ko H, Oh SJ, Kang J, Son JH, Lee K, Lee SW, Yoon HG, Suh JS, Huh YM, Haam S. Adv Funct Mater 2008;18:258–264.
73. Ago H, Kugler T, Cacialli F, Salaneck WR, Shaffer MSP, Windle AH, Friend RH. J Phys Chem B 1999;103:8116–8121.
74. Holzinger M, Abraham J, Whelan P, Graupner R, Ley L, Hennrich F, Kappes M, Hirsch A. J Am Chem Soc 2003;125:8566–8580. [PubMed: 12848565]
75. Kumar A, Mandal S, Selvakannan PR, Pasricha R, Mandale AB, Sastry M. Langmuir 2003;19:6277–6282.
76. Bruce IJ, Sen T. Langmuir 2005;21:7029–7035. [PubMed: 16008419]
77. del Campo A, Sen T, Lellouche J-P, Bruce IJ. J Magn Mater 2005;293:33–40.

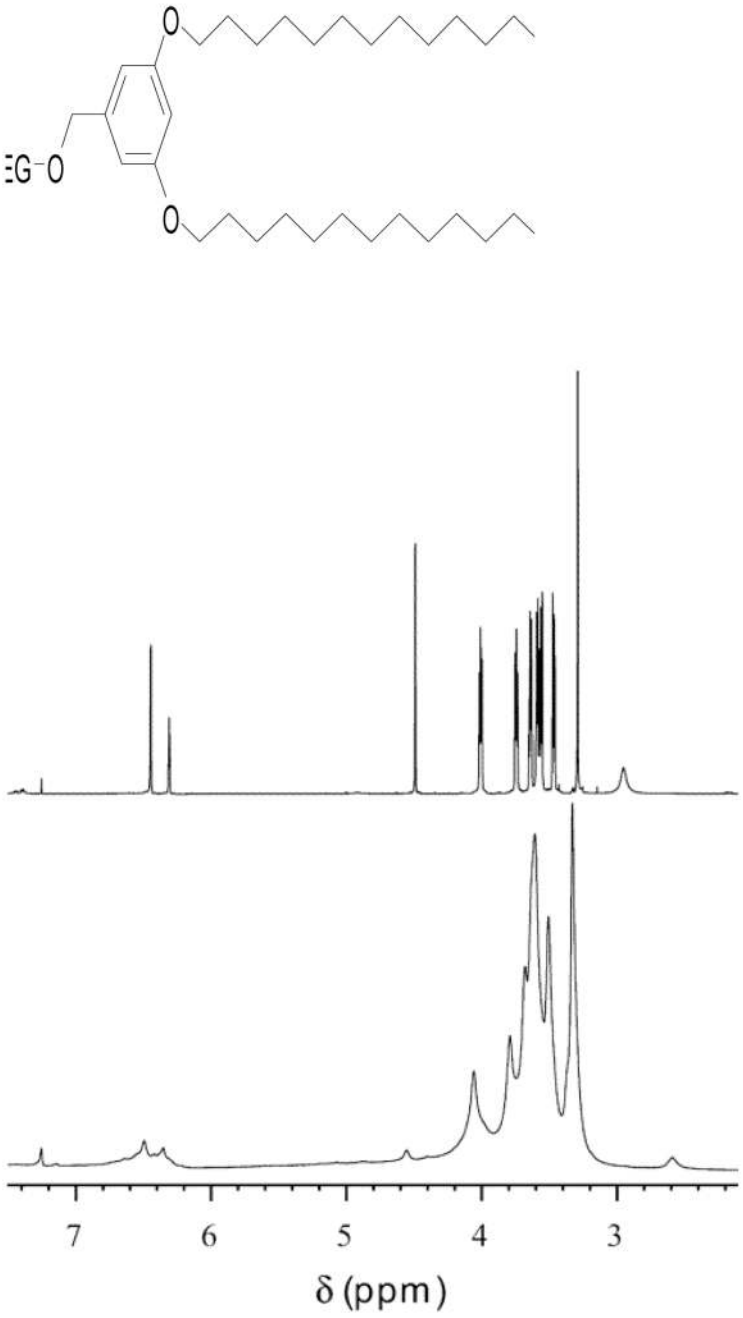

Figure 1.
^{1}H NMR spectra of the compound shown (top) and its SWNT-bound analog (bottom) in $CDCl_3$. (Reprinted with permission from [17], © 2002 American Chemical Society)

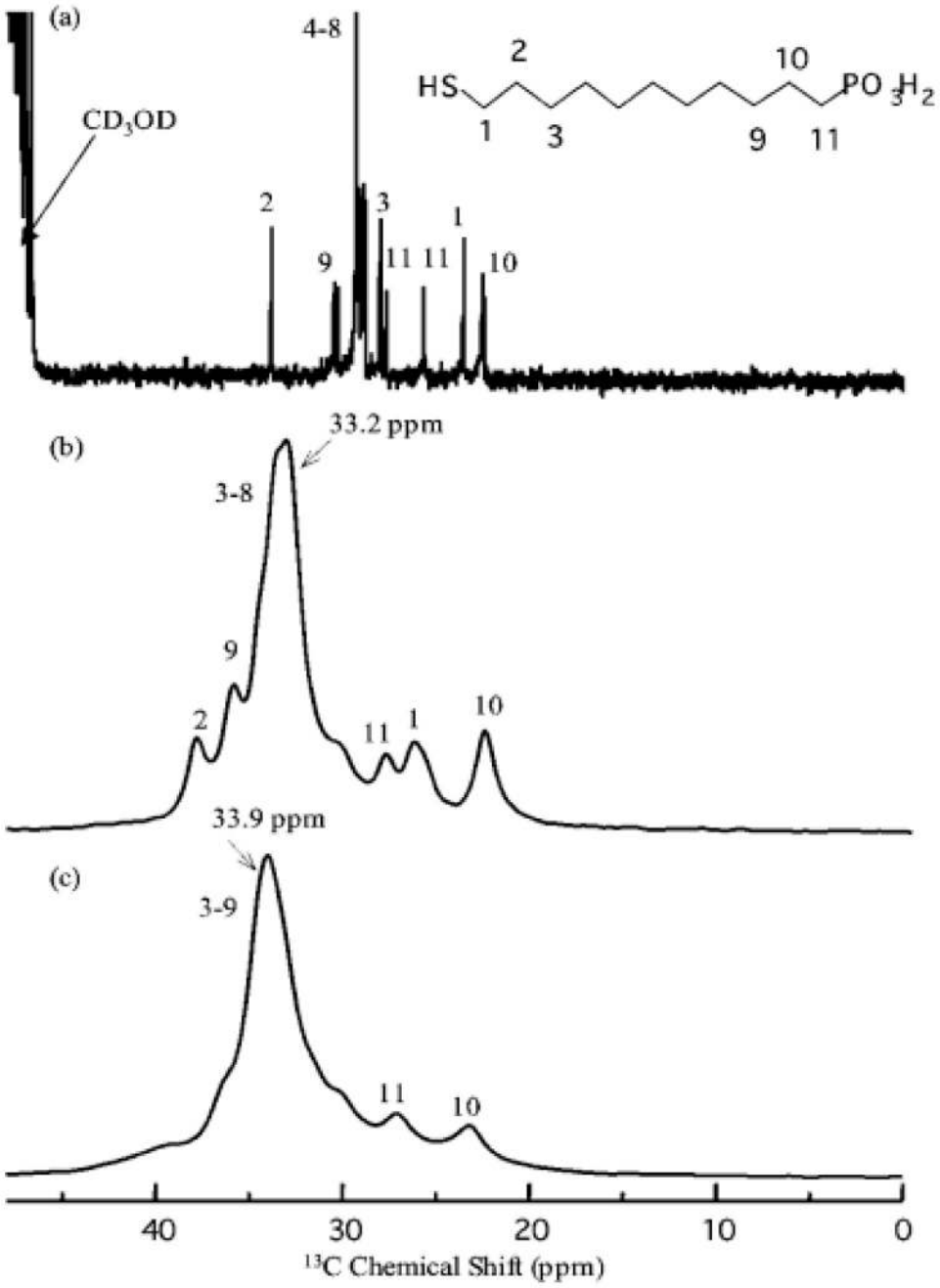

Figure 2.
^{13}C CP-NMR spectra of MUP (a) in methanol-d4, (b) in the solid state, and (c) on colloidal gold in the solid state. (Reprinted with permission from [34], © 2007 American Chemical Society)

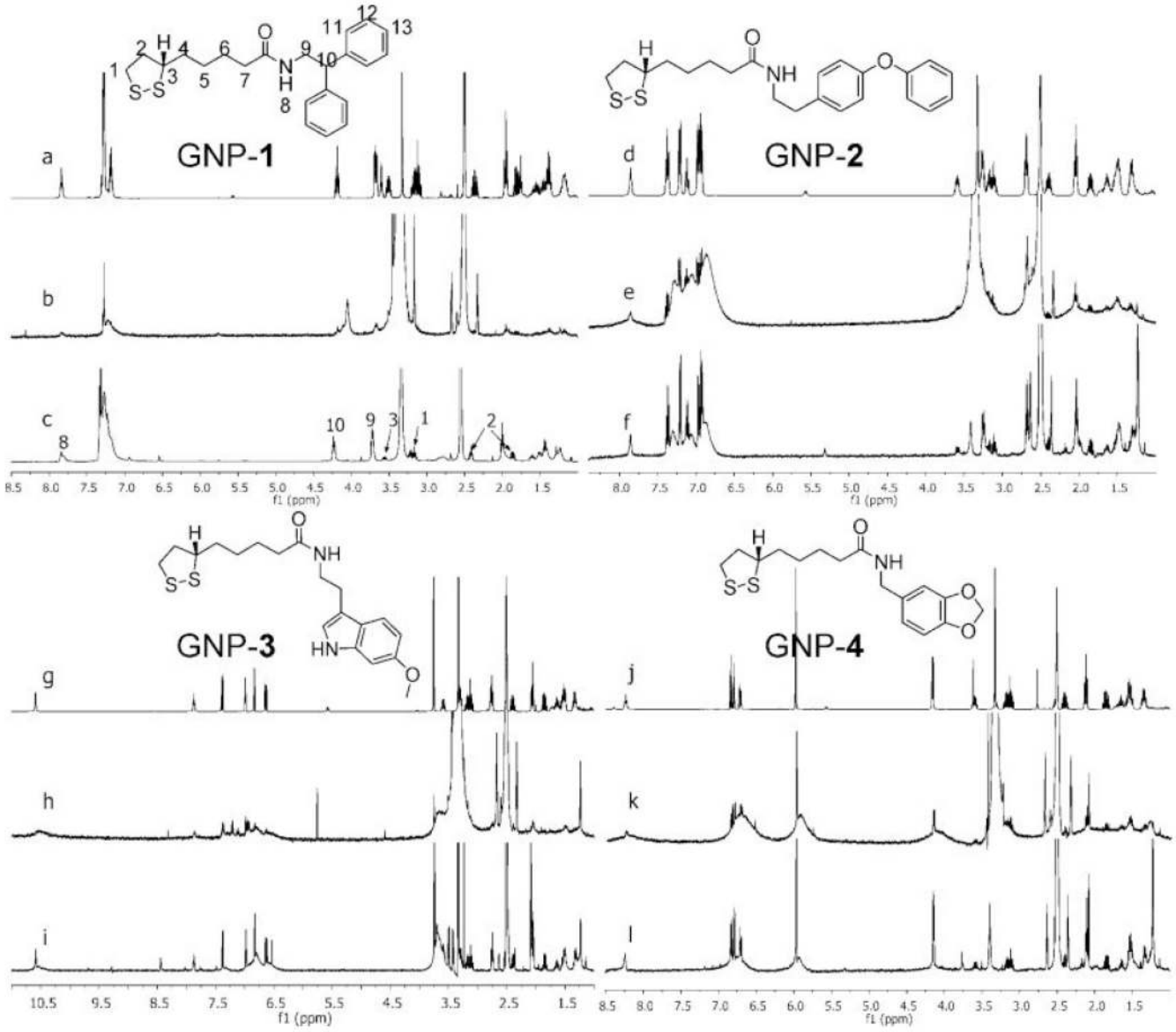

Figure 3.

^{1}H NMR spectra of free ligands 1–4 and GNP-1-4 in DMSO-d6. In each group, the top spectra (a, d, g, j) are the solution ^{1}H NMR spectra of free ligands (structures shown), the middle ones (b, e, h, k) are solution ^{1}H NMR spectra of corresponding GNPs and the bottom ones (c, f, i, l) are ^{1}H HRMAS NMR spectra. (Reprinted with permission from [58], © 2008 American Chemical Society)

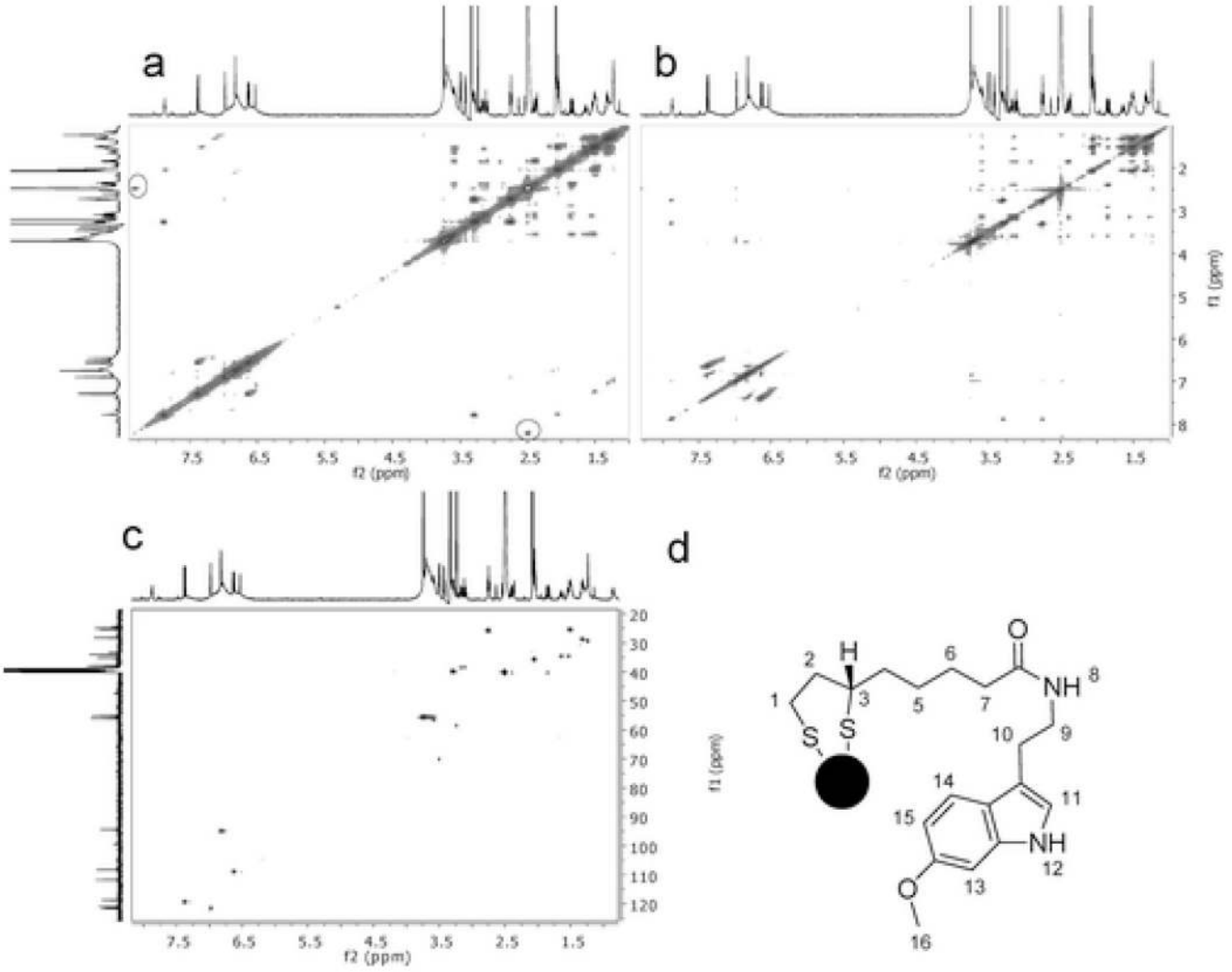

Figure 4.

HRMAS COSY (a), TOCSY (b), and HSQC (c) of GNP 3. 13C NMR spectrum shown vertically is from the free ligand because the ^{13}C HRMAS NMR spectra of GNPs were not able to obtain using nanoprobe (an inverse probe). Peaks inside the circled areas and those adjacent peaks in parallel to the diagonal line in panel a (upper left and lower right corners) are artifacts from spinning side bands. (Reprinted with permission from [58], © 2008 American Chemical Society)

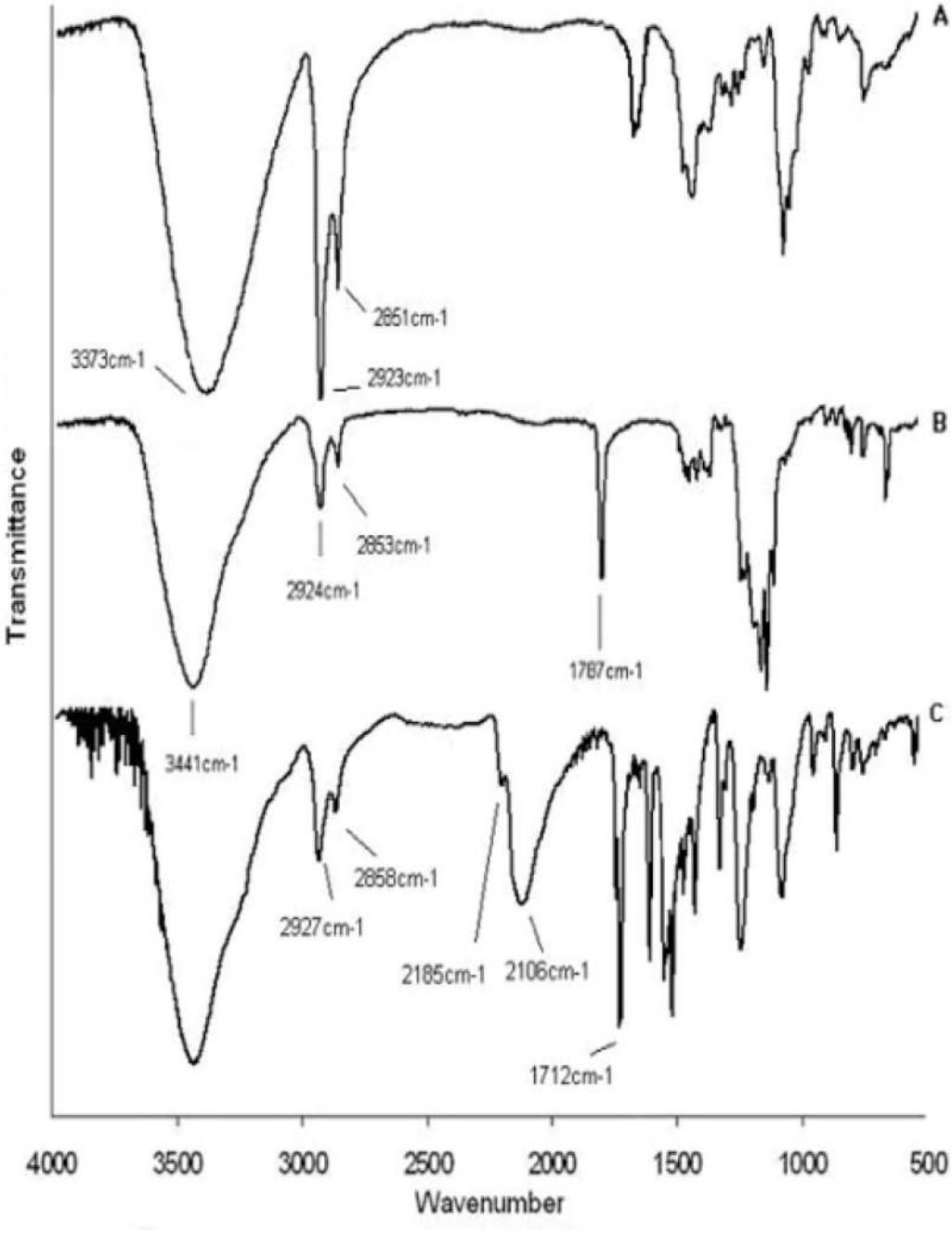

Figure 5.
Solid-state FTIR spectra of (A) Au-MCH nanoclusters and Au nanoclusters after derivatization with (B) CF_3COOH and (C) SCN-C_6H_4-NCO. (Reprinted with permission from [63], © 2006 American Chemical Society)

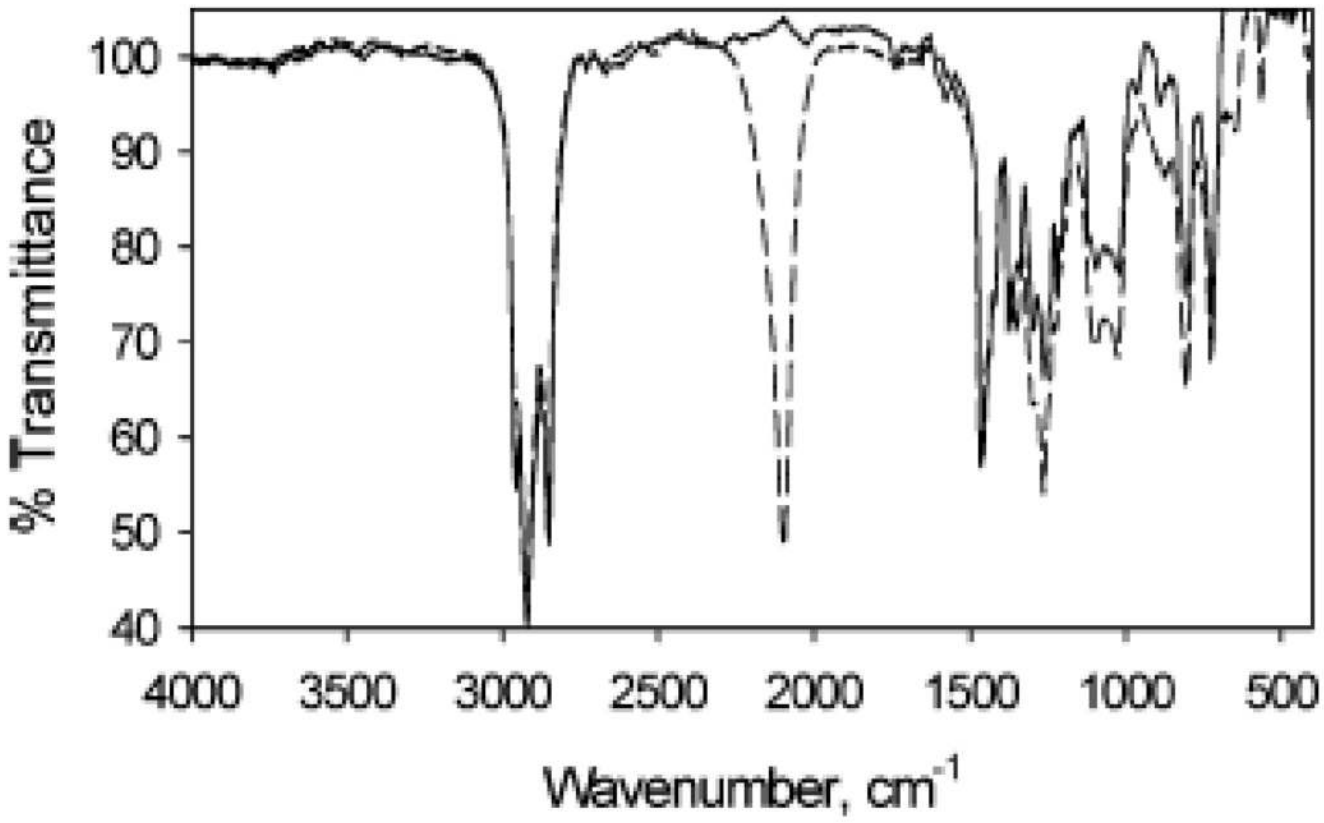

Figure 6.
FTIR spectra of the as-synthesized $C_{10}H_{21}SH$-modified Au particle (solid line) compared to azide-functionalized Au nanoparticles (dashed line). (Reprinted with permission from [27], © 2006 American Chemical Society)

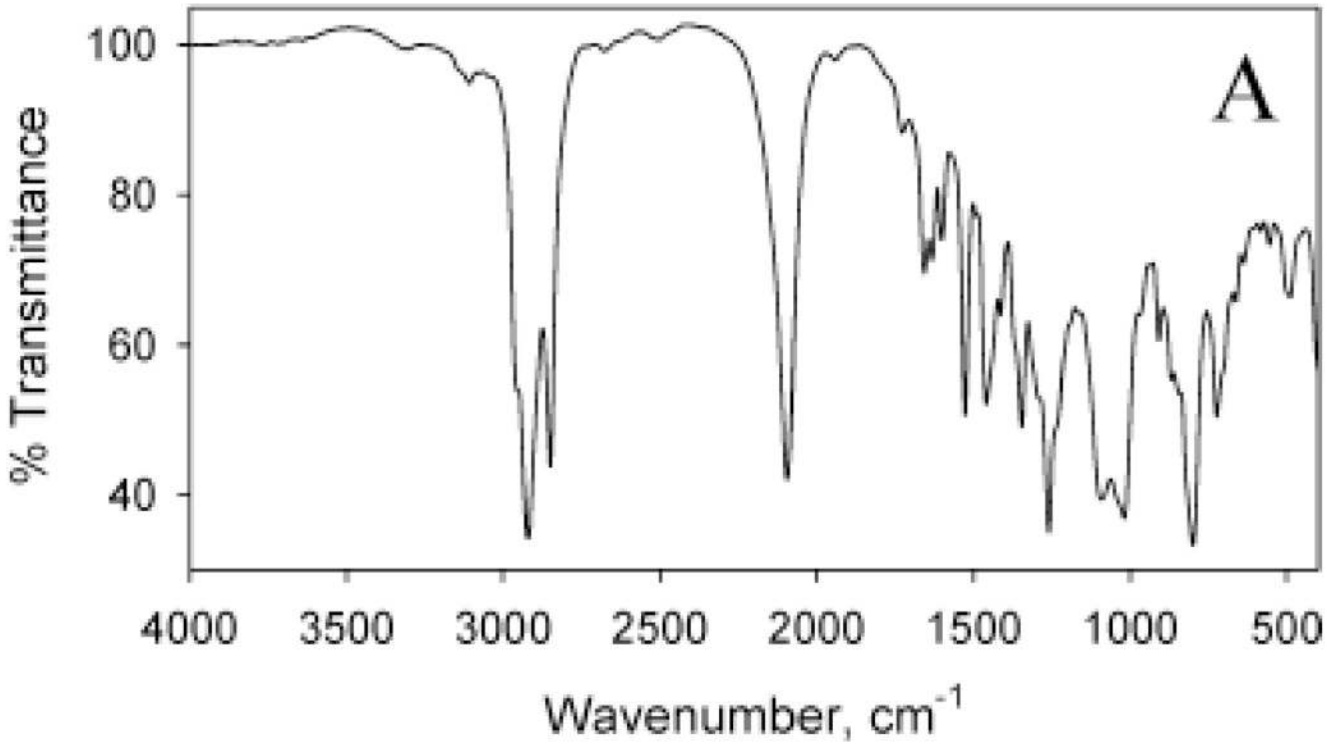

Figure 7.
FTIR spectra of Au nanoparticles following reaction with both Fc and NB alkynyl derivatives. (Reprinted with permission from [27], © 2006 American Chemical Society)

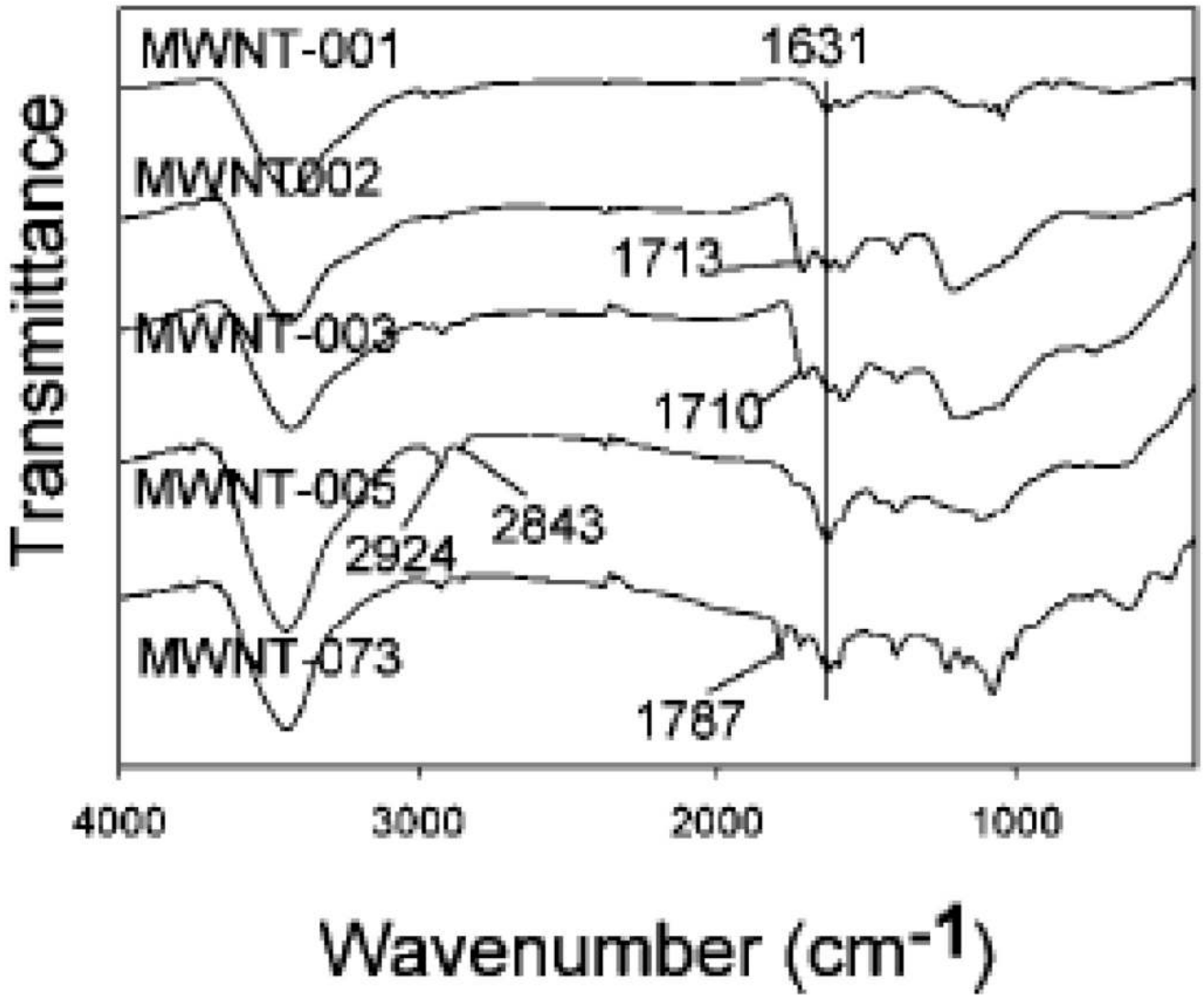

Figure 8.
is FTIR spectra of f-MWNTs **5**, **6**, **7**, **8**, and **9**. (Reprinted with permission from [6], © 2008 American Chemical Society)

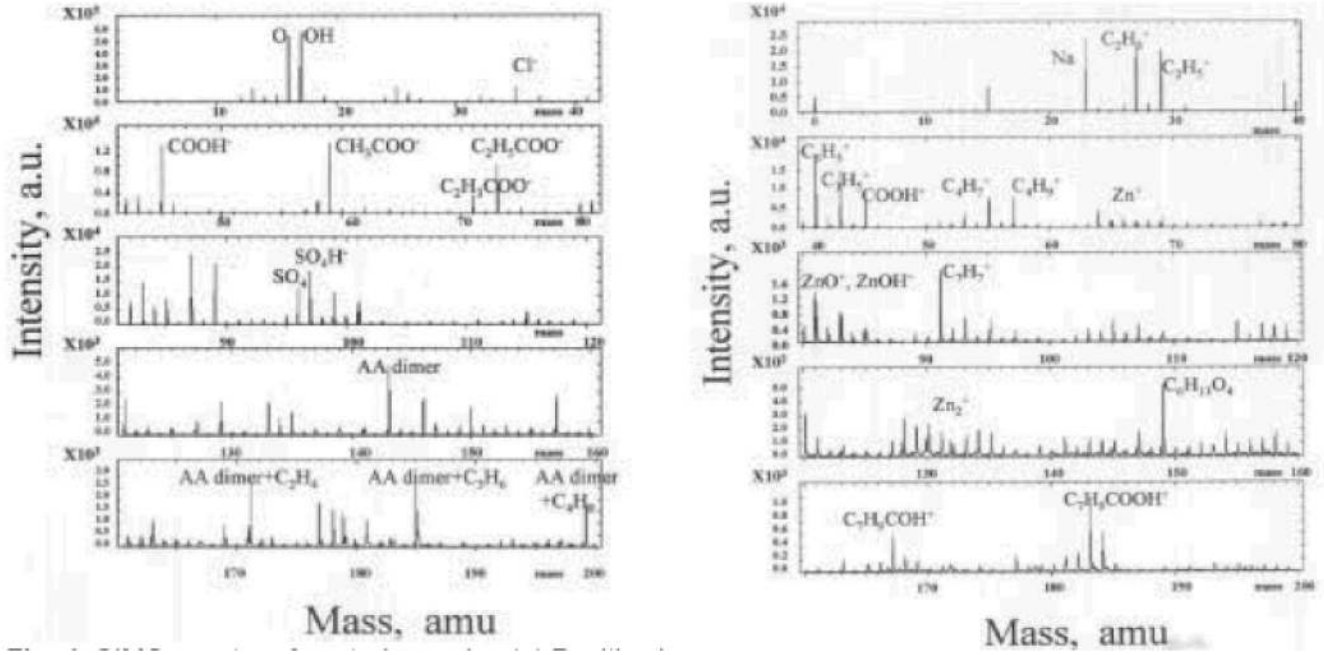

Figure 9.
TOFSIMS spectra of ZnO NPs coated with Acrylic acid (AA). (a) Positive image, (b) Negative image. (Reprinted with permission from [64], © 2004 Advanced Study Center Co., Ltd.)

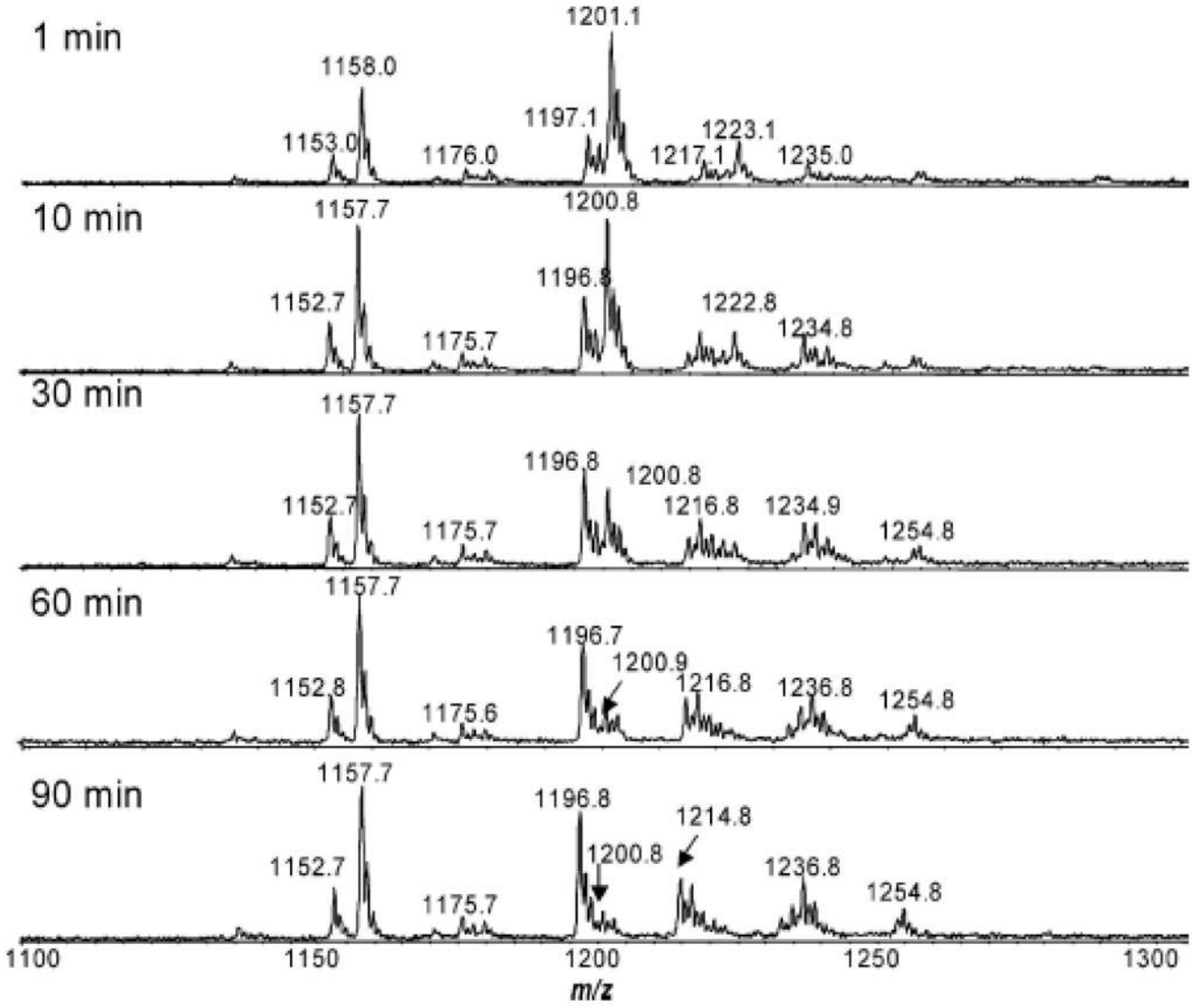

Figure 10.
Mass spectrum of p-βCD-SBH-$HAuCl_4$ reaction with time (1–90 min). (Reprinted with permission from [70], © 2008 American Chemical Society)

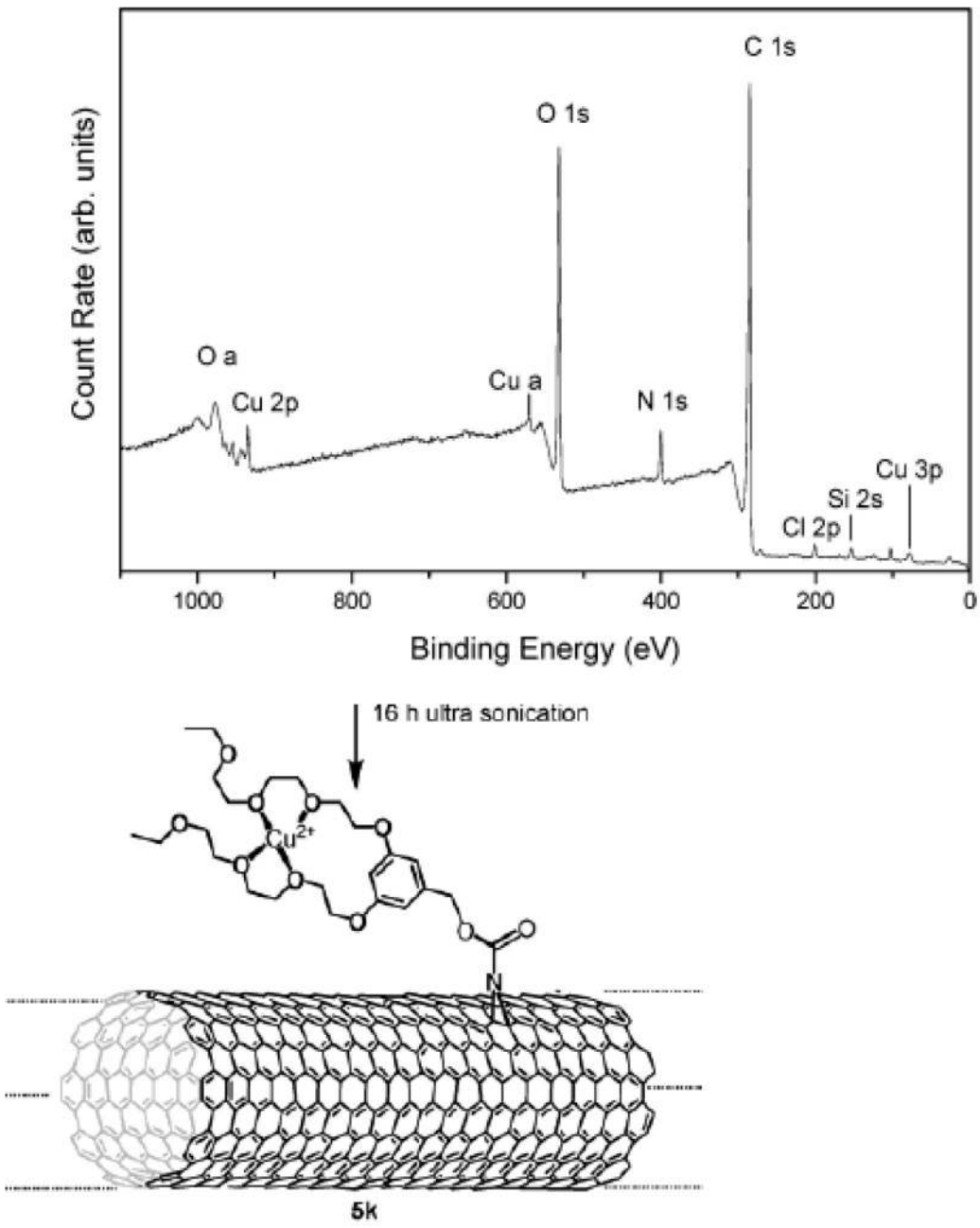

Figure 11.
XPS survey spectrum of 5k (structure see below). Composition: 69.1% C, 1.4% Si, 0.7% Cl, 4.4% N, 23% O, 1.4% Cu. (Reprinted with permission from [74], © 2003 American Chemical Society)

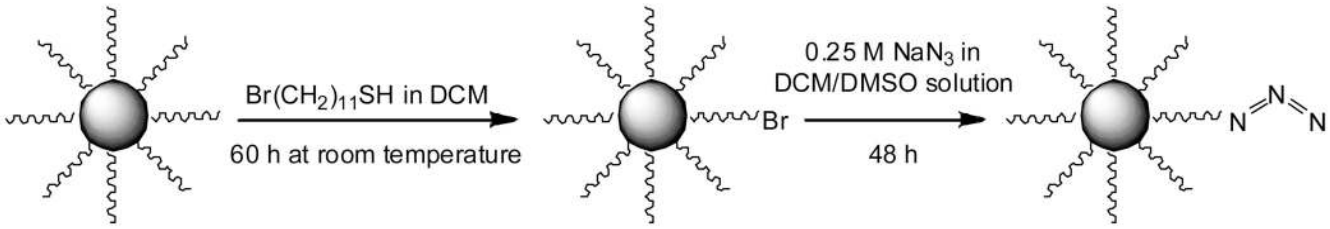

Scheme 1.
"Click" functionalization of Au NP surfaces.

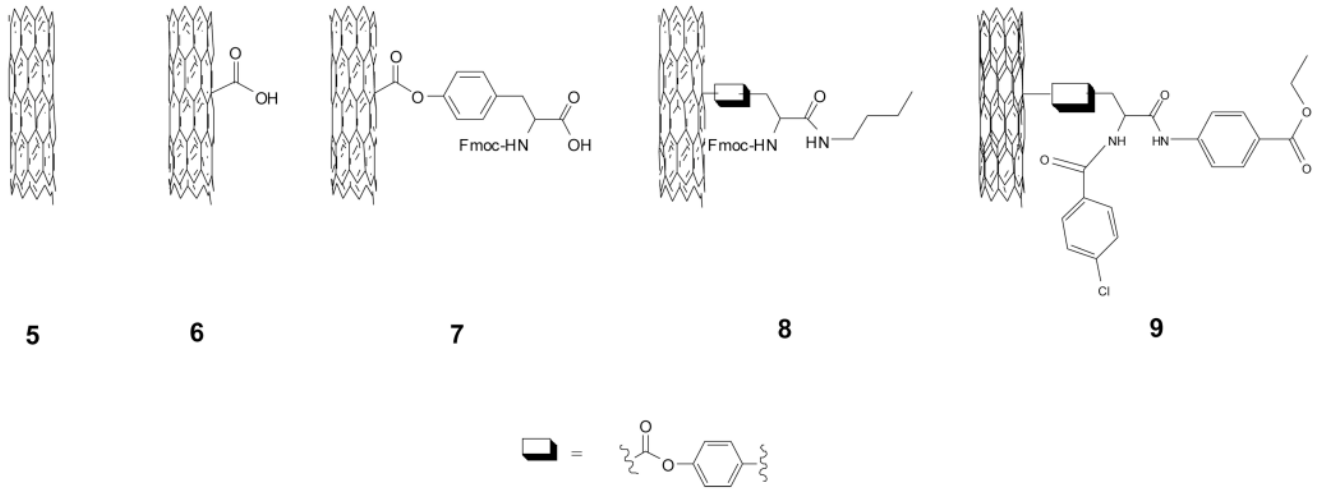

Scheme 2.
Structures of prinstine and four surface-modified MWNTs used in Figure 7.